trophilic substitution reactions on the position nature of the transition states;[17] the present work indicates the potential importance of the electron-distribution pattern within the σ complex type of transition state.

Experimental Section

Materials. Pentamethylbenzene and hexamethylbenzene were commercially available in high purity and were used without further purification. 1-Chloro-2,3,4,5,6-pentamethylbenzene was prepared by chlorination of pentamethylbenzene in nitromethane at 0°, using chlorine catalyzed with $ZnCl_2$, mp 154.5° (lit.[18] mp 155°). 1-Bromo-2,3,4,5,6-pentamethylbenzene was prepared by bromination of pentamethylbenzene with bromine in acetic acid at 25°, mp 161.2° (lit.[19] mp 160–162°). 1-Fluoro-2,3,4,5,6-pentamethylbenzene was prepared from 2,3,4,5,6-pentamethylaniline by the Schieman reaction, mp 72.5° (lit.[20] mp 59°). The pentamethylaniline was obtained by reduction of 1-nitro-2,3,4,5,6-pentamethylbenzene prepared by nitration of pentamethylbenzene with the nitrating agent described by Olah and Lin.[21]

Nitronium tetrafluoroborate was prepared according to the procedure of Olah and Kuhn[22] or the modified procedure introduced by Kuhn.[23] Antimony pentafluoride was triply distilled before preparation of the (1:1 *M*) HF–SbF_5 solution. Fluorosulfuric acid was doubly distilled before use.

Nmr Study of Ions. The benzenium and nitrobenzenium ions were prepared as described in the text and then were transferred by precooled pipets, or by direct pouring, to precooled nmr tubes. Proton spectra were obtained with a Varian Associates Model A56/60 spectrometer equipped with a variable-temperature probe. External TMS (capillary tube) was used as reference. Carbon-13 spectra were obtained on a Varian Associates Model XL-100 spectrometer, using ^{13}C-enriched TMS (capillary tube) as reference.

Acknowledgment. Support of our work by a grant of the U.S. Army, Office of Research, Durham, N.C., is gratefully acknowledged.

(18) A. Töhl, *Ber.*, **25**, 1524 (1892).
(19) T. Beacall, *Trans. Faraday Soc.*, **41**, 472 (1945).
(20) B. S. Biggs, U.S. Patent 2361591 (Oct 31, 1944); *Chem. Abstr.*, **39**, 2297 (1945).
(21) G. A. Olah and H. C. Lin, *Synthesis*, 488 (1973).
(22) S. J. Kuhn and G. A. Olah, *J. Amer. Chem. Soc.*, **83**, 4564 (1961).
(23) S. J. Kuhn, *Can. J. Chem.*, **45**, 3207 (1967).

Dynamical Study of Mechanistic Details in Organic Reactions. I. A Two-Step Study of Isomerizations of Cyclopropane-Type Molecules

Yves Jean and Xavier Chapuisat*

Contribution from the Laboratoire de Chimie Théorique[1] (490), Université de Paris-Sud, Centre d'Orsay, 91405 Orsay, France. *Received June 24, 1974*

Abstract: A brief explanation is presented for the results of experimental and theoretical investigations of geometrical and optical isomerizations of substituted cyclopropanes. In particular, the results of *ab initio* quantum mechanical calculations of the potential-energy surfaces for these reactions (notably in geometries of the transition states and suitability of static reaction paths) have shown the important fact that the reactions proceed roughly in sequence: ring opening, rotation of the terminal groups in the diradical species, and ring closure. In connection with these results, a preliminary dynamical study of the mechanism has been carried out in which the coupled rotations of the two terminal methylene groups on the trimethylene diradical and then the symmetric ring closure (or ring opening) of trimethylene (or cyclopropane) to cyclopropane (or trimethylene) are studied separately. The rotation surface is rather flat. Consequently, the possible trajectories are quite diverse, and only a few of them follow the previously proposed static-reaction paths. On the contrary, for ring closure the surface is very steep and the actual trajectories appear to deviate only slightly from the static path. The influence of different substituents on the trajectories is briefly investigated.

The theoretical investigation of a chemical reaction is essentially a two-step study. The first step is *static*. It consists in computing the potential energy of the reaction system as a function of the different geometrical parameters. Hence, some information on the reaction mechanism can be obtained, such as (i) the *minimum-energy path* to go from reactants to products and consequently the shape of the *reaction coordinate;* (ii) the difference between the calculated energies for the reactants and for the system at the *transition state*, which is compared to the *activation energy* of the reaction as a first approximation. In recent years, the growth of scientific computers as well as the realization of fast programs for quantum mechanical calculations has made the extensive investigation of potential-energy surfaces possible, for many organic reactions involving rather complex molecules.

The second step is of a *dynamical* nature. It consists in obtaining dynamical trajectories on the potential surface. Classical mechanics is supposed to describe correctly the atomic motion. In certain cases, such a study, at the end, allows the obtaining of the rate constant of the reaction. This was done for the first time by Karplus, Porter, and Sharma for the exchange reaction $H + H_2 \rightarrow H_2 + H$.[2] In other respects, the dynamical study brings new information on the mechanism of the reaction. Thus, Polanyi and Wong[3] studied the relative influence of initial translational

(1) The Laboratoire de Chimie Théorique is part of the Laboratoire de Physico-Chimie des Rayonnements associated with the CNRS.
(2) M. Karplus, R. N. Porter, and R. D. Sharma, *J. Chem. Phys.*, **43**, 3259 (1965).
(3) J. C. Polanyi and W. H. Wong, *J. Chem. Phys.*, **51**, 1439, 1451 (1969).

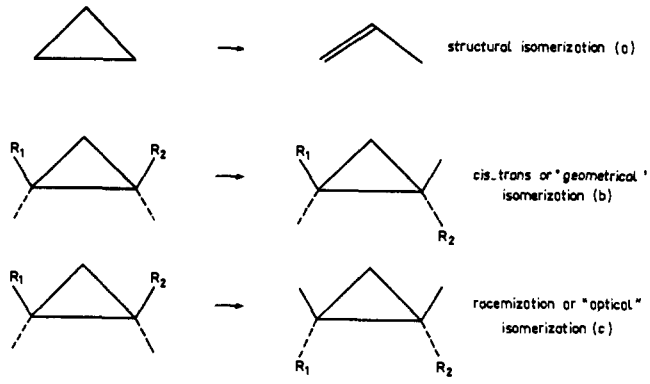

Figure 1.

energy and vibrational energy for the exchange reaction $A + BC \rightarrow AB + C$ as well as the final distribution of energy among the products. Such results cannot be derived from the only study of the static potential surface. Moreover, the dynamical study is sometimes clearly indispensable to elucidate a reaction mechanism. Thus the reaction $H_2 + I_2 \rightarrow 2HI$ was considered for a long time as a bimolecular reaction. Semiempirical calculations of the potential-barrier height for a bimolecular process gave a result of 42 kcal/mol,[4] an excellent agreement with the experimental value of the activation energy (41 kcal/mol). However, dynamical trajectories calculations using the same surface led to an activation energy of 53 kcal/mol.[5] Therefore a supplementary energy barrier of 11 kcal/mol exists, due exclusively to dynamical effects, and which practically excludes the bimolecular mechanism.

Complete dynamical studies, including the calculation of macroscopic reaction rates, have been restricted, until now, to triatomic or tetraatomic systems.[6] They require a preliminary knowledge of all the regions of the potential surface that are accessible for a given total energy. In addition, very many dynamical trajectories must be computed for suitably selected sets of initial conditions. For larger systems—even the smallest systems of interest in organic chemistry—it is impossible to obtain reaction rates by means of a complete dynamical study. Too many degrees of freedom have to be taken into account to obtain the full potential surface. Simplifying assumptions are required to scan this surface. In general, only those geometrical parameters which contribute notably to the reaction path are varied. The secondary parameters are either held constant or varied in a conventional way. There is no choice but to carry these constraints over into the dynamical calculation. Then the system is said to be constrained. Consequently, the vibrational excitation of purely nonreactive modes is ignored. From a static point of view, this is not a severe restriction if the important parameters have been carefully selected. On the contrary, from a dynamic point of view, the *a priori* neglect of any energy transfer between reactive and nonreactive modes (as well as the possible dissipation of a part of the energy over various nonreactive modes) can play a crucial role, in particular near the middle of the reaction where the final outcome of the reaction is decided.

Nevertheless, the dynamical study of the elementary processes occurring in the course of a reaction remains useful and complementary to the static study of the potential surface, even though it is incomplete and does not lead to the reaction rate. In particular, the comparison of dynamical trajectories with the static minimum-energy path is very instructive. Initial conditions seem to play a crucial part in the shape of dynamical trajectories. In a first study devoted to the dynamics of organic reactions, Wang and Karplus[7] have recently shown that for the reaction $CH_2 + H_2 \rightarrow CH_4$, only certain specific initial conditions lead to trajectories close to the minimum-energy path; most dynamical trajectories are much more complex than this path. Furthermore, deviations may result from the fact that for a given potential surface in two dimensions, which is represented as a map, the optimum path is most often drawn approximately under the assumption that the evolution of the system can be represented by the sliding of a mass point on the potential surface. This model is generally improper for constrained systems.[8]

In the present article, the results of a preliminary study of geometrical and optical isomerization reactions of cyclopropane-type molecules are presented. These organic reactions are very simple and have previously been the subject of detailed static quantum-mechanical calculations in our laboratory.[9]

Experiments and Previous Theoretical Investigations

The pyrolysis of substituted cyclopropanes leads to three types of unimolecular isomerizations (see Figure 1). The first kinetic study of the conversion of cyclopropane into propylene (reaction a) was undertaken by Trautz and Winkler in 1922.[10] The geometrical isomerization was discovered by Rabinovitch, Schlag, and Wiberg in 1958;[11] reaction b is faster than the structural isomerization in propylene (a). Finally, the optical isomerization was observed, independently by Crawford and Lynch,[12a] by Berson and Balquist,[12b] and by Bergmann and Carter;[12c] their common conclusion states that geometrical (b) and optical (c) isomerizations are competitive reaction processes. This was confirmed recently by Doering and Sachdev.[12d] Most mechanisms for the geometrical and optical isomerization reactions invoke a trimethylene diradical species (Figure 2).

These reactions have aroused a great deal of interest among theoretical chemists. Indeed, they lie within the simplest reactions in organic chemistry; formally,

(4) L. M. Raff, L. Stivers, R. N. Porter, D. L. Tompson, and L. B. Sims, *J. Chem. Phys.*, **52**, 3449 (1970).
(5) R. N. Porter, D. L. Tompson, and L. B. Sims, *J. Amer. Chem. Soc.*, **92**, 3208 (1970).
(6) D. L. Bunker in "Methods in Computational Physics," Vol. 10, Academic Press, New York, N. Y., 1971, p 287, and references therein.
(7) I. S. Y. Wang and M. Karplus, *J. Amer. Chem. Soc.*, **95**, 8160 (1973).
(8) X. Chapuisat, Y. Jean, and C. Leforestier, to be submitted for publication.
(9) (a) Y. Jean, L. Salem, J. S. Wright, J. A. Horsley, C. Moser, and R. M. Stevens, *Pure Appl. Chem., Suppl.*, **1**, 197 (1971); (b) J. A. Horsley, Y. Jean, C. Moser, L. Salem, R. M. Stevens, and J. S. Wright, *J. Amer. Chem. Soc.*, **94**, 279 (1972).
(10) M. Trautz and K. Winkler, *J. Prakt. Chem.*, [2] **104**, 53 (1922). For the most recent experimental work on the mechanism of this reaction, see J. E. Baldwin, and M. W. Grayston, *J. Amer. Chem. Soc.*, **96**, 1629, 1630 (1974).
(11) B. S. Rabinovitch, E. W. Schlag, and K. W. Wiberg, *J. Chem. Phys.*, **28**, 504 (1958).
(12) (a) R. J. Crawford and T. R. Lynch, *Can. J. Chem.*, **46**, 1457 (1968); (b) J. A. Berson and J. M. Balquist, *J. Amer. Chem. Soc.*, **90**, 7343 (1968); (c) W. L. Carter and R. G. Bergman, *ibid.*, 90, 7344 (1968); R. G. Bergman and W. L. Carter, *ibid.*, **91**, 7411 (1969); (d) W. von E. Doering and K. Sachdev, *ibid.*, **96**, 1168 (1974).

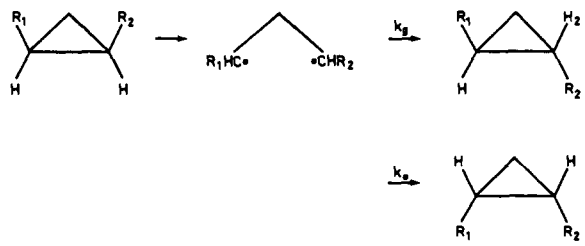

Figure 2. Mechanisms usually invoked for the geometrical and optical isomerization of cyclopropane-type molecules.

they require only a rotation of 180° in one or both methylene group. Otherwise, the nature as well as the chemical behavior of the postulated intermediate diradical creates problems to which nothing definitely satisfactory has been answered.[13] After the preliminary theoretical work on the trimethylene diradical by Hoffmann,[14] several groups undertook nonempirical quantum-mechanical calculations on (i) the ring opening of the cyclopropane molecule and (ii) the rotations of the terminal methylene groups in the diradical species thus obtained.[9,15] The results of these calculations confirm the competition experimentally observed between the two isomerization reactions. Moreover, no potential-energy barrier is found in the ring closure of the diradical toward the cyclopropane (the second step in the reaction of Figure 2). Finally, the geometry of the transition state for geometrical isomerization has been resolved in 21-dimensional space, and that for optical isomerization obtained approximately.[9] Static reaction paths were proposed for both reactions b and c.

General Considerations on the Dynamical Study

The potential-energy surface that is used in the following study was computed by one of us.[9] It is necessary to recall the method which we used in this static investigation since the preliminary dynamical description presented below lies within the same scheme.

The static study required consideration of three main geometrical parameters: the angle of ring opening CCC and the rotation angles for both terminal methylene groups. First, the potential-energy surface was investigated under the assumption that the ring-opening motion and the rotations were decoupled. In other words the ring opening from the cyclopropane to the face-to-face diradical FF (*cf.* Figure 3a) is carried out first. Next, various reaction paths, along which FF is transformed into either its geometrical or its optical isomer are investigated. These paths go through symmetric halfway points,[16] such as EF (edge-to-face, *cf.* Figure 3b) and EE (edge-to-edge, *cf.* Figure 3c). It is worthwhile to note that they all have very nearly the same opened-ring angle, namely about 113°. Within this scheme,

(13) For a very complete review, see R. G. Bergman in "Free Radicals," J. K. Kochi, Ed., Wiley-Interscience, New York, N. Y., 1973.

(14) R. Hoffmann, *J. Amer. Chem. Soc.*, **90**, 1475 (1968).

(15) (a) R. J. Buenker and S. D. Peyerimhoff, *J. Phys. Chem.*, **73**, 1299 (1969); (b) A. K. Q. Siu, W. M. St.-John, II, and E. F. Hayes, *J. Amer. Chem. Soc.*, **92**, 7249 (1970); (c) P. J. Hay, W. J. Hunt, and W. A. Goddard, III, *ibid.*, **94**, 638 (1972).

(16) Some paths, for which the symmetry constraints at halfway are lifted, were also studied. However, this did not modify significantly the conclusions drawn from the previous symmetric paths studies. In the present article, we refer only to the results for symmetric reaction paths.

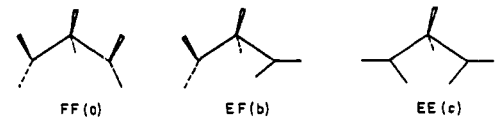

Figure 3. Definition of the geometries of the three diradicals face-to-face (FF), edge-to-face (EF), and edge-to-edge (EE).

typical reaction paths for both geometrical and optical isomerizations therefore are

cyclopropane ⟶ FF ⟶ EF ⟶ FF ⟶ cyclopropane (geometrical isomer)

cyclopropane ⟶ FF ⟶ EE ⟶ FF ⟶ cyclopropane (optical isomer)

The theoretical search according to the minimum-energy path criterion leads respectively to EF (geometrical isomerization) and to a structure very close (both in energy and in conformation) to EE (optical isomerization) as transition states. These diradical structures have similar energy.

The reaction paths thus obtained are not absolute minimum-energy paths on the full surface since the isomerizing molecule has been constrained to go through the intermediate structure FF. Complementary calculations show that variation of the CCC angle simultaneously with the rotation of the methylene groups modifies only very slightly the results. The rotation of one (or both) methylene group(s) remains very difficult energetically, unless the ring is opened sufficiently[17] with a narrow range of permissible CCC angles.

Our dynamical study is based on similar assumptions concerning the coordinates and their coupling. In a first step, the dynamics of the ring closure (FF → cyclopropane) and the rotations in the trimethylene diradical have been investigated separately. The results of this preliminary study are those of the present article. In a future publication, we will present results including explicitly the coupling of methylene rotation with CCC angle bending.

It is important to remark that the decoupling of these two motions may be a mistake in the dynamical approach, even though it is satisfactory as a first approximation in the static approach. The aforementioned neglect of vibrational energy transfer to nonreactive modes (and, even here, between reactive modes) may be particularly damaging. However, we present here detailed dynamic information on both steps of the reaction separately.

In particular, we have obtained: numerous dynamical trajectories with characteristics which distinguish them strongly from the (static) minimum-energy paths; and relative times for the ring opening and for methylene rotation and the variation of these times with the mass of the rotating terminal groups. This leads to a dynamical analysis of substituent effects.

We have also developed elsewhere[8] a theoretical treatment for the analytical description of numerical potential-energy surfaces and the derivation of general equations for the mechanics of constrained systems.

(17) Y. Jean, Thèse de Doctorat d'Etat, Université de Paris-Sud, Centre d'Orsay, 1973.

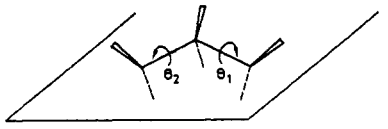

Figure 4. Definition of the two rotation angles of the terminal groups around the adjacent carbon–carbon bonds.

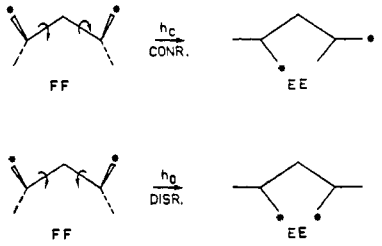

Figure 5.

Rotation of the Terminal Methylene Groups in the Trimethylene Diradical

1. Description and Parametrization of the Potential Energy Surface. Our original static study[9] led to a numerical two-dimensional potential-energy surface. It represents the potential energy of the diradical as a function of the two rotation angles (θ_1 and θ_2) of the terminal methylenes (see Figure 4). This surface exhibits the following characteristics. The most stable structure is that of the diradical FF ($\theta_1 = \theta_2 = 0$). The energies of the diradicals EF ($\theta_1 = 90°$, $\theta_2 = 0$) and EE ($\theta_1 = \theta_2 = 90°$) are close to each other; EE is, however, slightly more stable than EF. The transformation of EF into EE requires no activation energy. The conrotatory and disrotatory concerted motions which transform FF into EE (see Figure 5) travel through potential-energy barriers, respectively equal to h_C and h_D. Quantum mechanical calculations show the conrotatory motion to be energetically easier than the disrotatory one ($h_C < h_D$).[14] We now require an approximate description of this surface by an analytical expression, which is simple but yet retains the essential features (cols, valleys, etc.) of the surface. There are four main features of the surface which the analytic formula must reproduce accurately: the energies of the half-way points EF and EE, respectively denoted by h_1 and h_2; the potential-barrier heights, h_C and h_D, respectively for conrotatory and disrotatory rotations. The following analytic formula is somewhat arbitrary; it is selected because it abides by the law of symmetry and takes into account the four parameters, independently

$$V(\theta_1,\theta_2) = a \sin^2(\theta_1 + \theta_2) \sin^2(\theta_1 - \theta_2) + b \sin^2(\theta_1 - \theta_2) \cos^2(\theta_1 + \theta_2) + c \sin^2(\theta_1 + \theta_2) \cos^2(\theta_1 - \theta_2) + d \sin^2\theta_1 \sin^2\theta_2$$

According to this formula, the potential energy of the diradical FF is chosen as origin of energies. The expressions of the parameters a, b, c, and d as functions of h_1, h_2, h_C, and h_D are

$$a = h_1$$
$$b = (h_D + (h_D^2 - h_D h_2)^{1/2})/2$$
$$c = (h_C + (h_C^2 - h_C h_2)^{1/2})/2$$
$$d = h_2$$

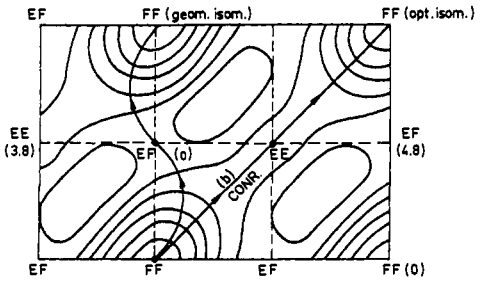

Figure 6. Static reaction paths on a two-dimensional potential-energy surface for the (a) geometrical and the (b) optical isomerizations. The energies (expressed in kcal/mol) are relative to the internal energy of the configuration FF taken as zero. The energy gap between two isoenergetic lines is 0.8 kcal/mol.

The number of parameters introduced is too small to prescribe independently the *heights* and the *positions* of the conrotatory and disrotatory barriers. Thus, the values of h_1, h_2, h_C, and h_D used below do not match rigorously those computed for the symmetric surface.[9a] They are slightly modified so that the surface as a whole is qualitatively well fitted, and the energy barriers are correctly localized. The values selected are as follows

$$h_1(\text{EF}) = 4.8 \text{ kcal/mol (calcd: 5.1)}$$

$$h_2(\text{EE}) = 3.8 \text{ kcal/mol (calcd: 3.7)}$$

$$h_C = 4.0 \text{ kcal/mol (calcd: 3.9)}$$

(position of the maximum of the barrier is 64.7° after FF, instead of 65° on the computed surface)

$$h_D = 5.5 \text{ kcal/mol (calcd: 5.5)}$$

(position of the maximum of the barrier is 53.3° after FF, instead of 53.5° on the computed surface).

In Figure 6, the parametrized potential surface is represented along with the static paths for both isomerizations.

2. Equations of Motion and Initial Conditions. The nuclear motion on the potential surface is described within the framework of classical mechanics. The initial state is described classically; *i.e.*, the energy of the system as well as the distribution of this energy over the different modes of distortion are varied in a continuous way. A supplementary simplification is introduced in the mechanical description of the system. In the optimized geometries of diradicals EF and FF, the "face" (F) methylene groups are pyramidalized toward the inner part of the ring.[9] Rotations of these groups by 90° occur through a progressive depyramidalization on the static surface. In the static calculations, the depyramidalization angles (denoted by β_1 and β_2) were not taken as independent variables, but rather as functions of θ_1 and θ_2. Thus the computed potential-energy function V, and its parametrized version, is really of the form $V(\theta_1, \theta_2, \beta_1(\theta_1,\theta_2), \beta_2(\theta_1,\theta_2))$. Although the pyramidalization motion is not free (adiabatic adjustment motion), it contributes slightly to the kinetic energy of the system. Here it is neglected; the kinetic energy of the system is formally written by taking into account only the principal twisting motion (θ), as if both methylene groups remained trigonal throughout the rotations.

Under these conditions, the Lagrangian equations for the system are

$$I\dot{\theta}_1 = -\partial V/\partial\theta_1$$
$$I\dot{\theta}_2 = -\partial V/\partial\theta_2 \quad (1)$$

where $I = 2m_H R_{C-H}^2 \sin^2(\gamma/2)$ and $\gamma = \angle HCH$. γ is supposed to be constant. These two second-order differential equations transform into four first-order differential equations by the following change of variables: $\theta_1 = y_1$, $\theta_2 = y_2$, $\dot{\theta}_1 = y_3$, and $\dot{\theta}_2 = y_4$. Thus, the system of coupled equations is explicitly shown in eq 2. The

$$\dot{y}_1 = y_3$$
$$\dot{y}_2 = y_4$$
$$\dot{y}_3 = \{-2a \sin(y_1 + y_2) \sin(y_1 - y_2) \sin 2y_1 - [2b \sin(y_1 - y_2) \cos(y_1 + y_2) + 2c \sin(y_1 + y_2) \cos(y_1 - y_2)] \cos 2y_1 - d \sin^2 y_2 \sin 2y_1\}/I \quad (2)$$
$$\dot{y}_4 = \{2a \sin(y_1 + y_2) \sin(y_1 - y_2) \sin 2y_2 - [2c \sin(y_1 + y_2) \cos(y_1 - y_2) - 2b \sin(y_1 - y_2) \cos(y_1 + y_2)] \cos 2y_2 - d \sin^2 y_1 \sin 2y_2\}/I$$

numerical integration of (2) requires four initial conditions and then leads to a particular trajectory. The initial conditions are: (i) The initial angular positions of both rotors (θ_1^0 and θ_2^0). Since here the motions of ring opening and rotations are separated, the positions corresponding to diradical FF are always selected as $\theta_1^0 = \theta_2^0 = 0$. This assumes implicitly that the rotational motion does not initiate during the first step of the reaction when the CCC angle opens from 60°, until about 113°. Clearly, a more realistic description would require taking into account an entire distribution of initial positions θ_1^0, θ_2^0 around $\theta_1^0 = \theta_2^0 = 0$. Such explicit introduction of the coupling between methylene rotation and ring opening is considered in the next paper.

(ii) The total initial (rotational) energy E_0. Here, trajectories have been run for initial energies in the range 4.81–5.80 kcal/mol; *i.e.*, our study has been restricted to the dynamical behavior of diradicals possessing an internal energy slightly greater than that of the transition states. This behavior is expected to be very sensitive to the different potential-energy barriers (in position as well as in height).

(iii) The initial distribution of E_0 between the two rotors. This is characterized by the angle δ defined by

$$tg\delta = \dot{\theta}_1^0/\dot{\theta}_2^0$$

where $\dot{\theta}_1^0$ and $\dot{\theta}_2^0$ are the initial rotational velocities of the two groups. Then the relationship

$$\dot{\theta}_2^0 = \pm\cos\delta\{2I^{-1}[E_0 - V(\theta_1^0,\theta_2^0)]\}^{1/2}$$

is used. Symmetry considerations show that only the values of δ between $\delta_c = +45°$ (synchronous conrotatory motion) and $\delta_d = -45°$ (synchronous disrotatory motion) need be considered. The value $\delta = 0$ corresponds to all the initial energy being concentrated in a single rotor. The parameter δ is varied with a step of 2°; *i.e.*, 46 trajectories are studied for each value of the total energy.

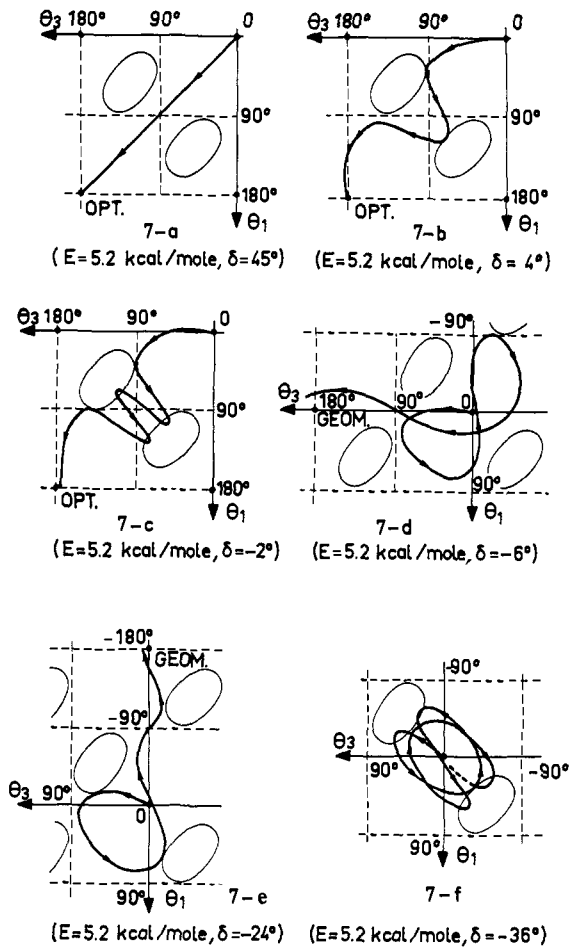

Figure 7. Some typical trajectories plotted on the potential-energy surface of Figure 6. Here, the surface is symbolically represented by only the $V = 4.9$ kcal/mol energy contour.

The only true dynamical variables in the present study are the two angles of rotation (θ_1 and θ_2). Hence, the computed trajectories are endless: the rotations can go on indefinitely with continual energy transfer between the two rotors. In the real molecule, the rotations stop whenever the cyclization (ring closure) occurs.

3. Results. (a) Typical Trajectories. The trajectory in Figure 7a has been calculated for two rotors with the same initial velocity ($\delta = \delta_c = 45°$). The initial kinetic energy (5.2 kcal/mol)[18] is greater than the conrotatory potential-energy barrier (4.0 kcal/mol). The optical isomer is formed. Since the starting point ($\theta_1^0 = \theta_2^0 = 0$) lies at the bottom of the "conrotatory valley," the reaction path is a straight line. Thus the dynamical path is the same as the static minimum-energy path. It should be emphasized that $\delta = \delta_c$ is the only value for which such a result is observed. The optical isomer is formed after 1.4×10^{-13} sec.

In Figures 7b and 7c, the trajectories correspond to $\delta = +4°$ and $\delta = -2°$, respectively. The minimum-energy path is not followed anymore by the molecule. However, since the dynamical energy still exceeds the potential-energy barrier h_C by 1.2 kcal/mol, the optical isomer is still reached, although the deviations of the trajectories with respect to the minimum-energy path become more and more important. The trajectory in

(18) All energies are measured from open cyclopropane FF ($V(0,0) = 0$).

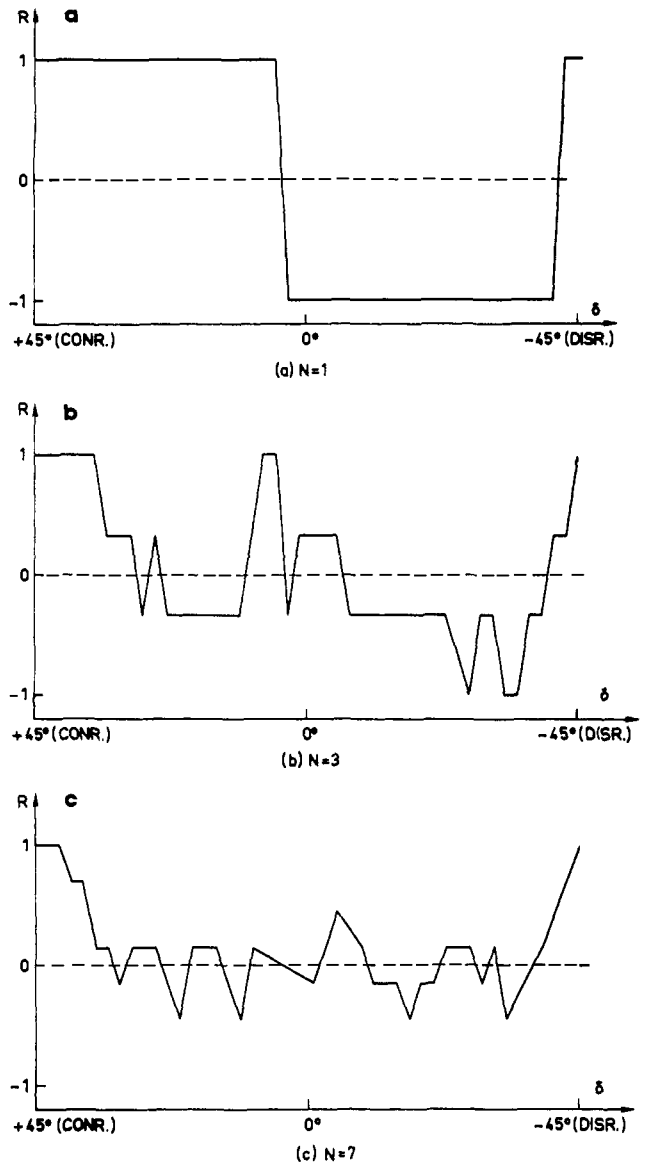

Figure 8. Plot of the ratio, R = ([cis] − [trans])/N, where N is the number of isomers successively formed, *vs.* δ, the initial distribution of the excess energy among the two rotors, for (a) N = 1, (b) N = 3, and (c) N = 7.

Figure 7c is the limiting case; *i.e.*, $\delta = -2°$ is the limiting value for which the optical isomer is directly formed. Interestingly, the representative point of the molecule finds the right pathway by bouncing off the two disrotatory bumps surrounding the conrotatory valley several times in the course of the motion. That part of the kinetic energy which corresponds to a distortion along the reaction coordinate is very small and just sufficient to go through the transition state. The remaining kinetic energy is wasted in motions perpendicular to the main pathway axis. It is worthwhile to note that initially the energy was almost totally concentrated in one of the two rotors. On an intuitive basis, such a lopsided energy partition was expected to facilitate the formation of the geometrical isomer, the total energy (5.2 kcal/mol) being sufficient to go over the transition state (h_1 = 4.8 kcal/mol). As shown in Figure 7c, the representative point of the molecule comes extremely close to the transition state for geometrical isomerization. However, it does not go through this transition state because locally it moves along a coordinate which is almost perpendicular to that which is necessary to form the geometrical isomer. In other words, the molecule cannot use all its kinetic energy to jump over the saddle point. The time interval which is necessary to form the optical isomer increases for dynamical trajectories getting further and further away from the minimum-energy path: 3.0×10^{-13} sec for $\delta = 4°$ and 5.5×10^{-13} sec for $\delta = -2°$.

For $-30° < \delta < -4°$ and for E_0 = 5.2 kcal/mol, the reflection of the trajectories on the disrotatory bumps is strong enough to make the representative point of the molecule return to its starting point. Consequently, in their initial step, these trajectories are nonreactive. However, as the rotations are allowed to go on, the representative point goes on moving on the surface so that the molecule can, at some moment, reach the conformation of a transition state (subsequent steps). Then the geometrical isomer is formed most often. The passage of the col for geometrical isomerization occurs in two different manners: (i) along the disrotatory reaction coordinate, as would be expected from the static study[9] (*cf.* Figure 7d); (ii) along a different reaction coordinate, as in Figure 7e. This is possible because the energy in the molecule is greater than that of the transition state.

Finally, for $E_0 < 5.5$ kcal/mol and for values of δ close to $\delta_D = -45°$, *i.e.*, for an initial distortion of the molecule along the disrotatory mode, the trajectories are nonreactive throughout all the time range of the numerical integrations (1.2×10^{-12} sec). Such a trajectory for $\delta = -36°$ is pictured in Figure 7f.

(b) Influence of δ (Initial Distribution of the Energy) on the Nature of the Product Isomer. A detailed study of 46 trajectories at a given total energy (E_0 = 5.8 kcal/mol) is presented below. This value of E_0 is interesting (i) because, in principle, any point on the surface is attainable; but (ii) the excess energy with respect to the various potential barriers is small (1.8 and 1.0 kcal/mol with respect to h_C and EF, respectively). In the following, the reacting molecule is always supposed to be the cis isomer.

In Figure 8a, the nature of the first isomer formed is plotted as a function of δ. The value +1 corresponds to formation of the optical isomer and the value −1 to the geometrical isomer. For $\delta > 0$, the optical isomer is formed and the trajectories are of the types shown in Figures 7a, 7b, or 7c; *i.e.*, the representative point follows the conrotatory valley but with wider deviations with respect to the minimum-energy path. For $\delta < 0$ (initial disrotatory motion), the first isomer formed is the geometrical isomer. It is formed directly, without any intermediate return to starting geometry. The molecule is sufficiently energetic to cross over the saddle point, whatever the local coordinate is. When δ is close to −45°, the optical isomer is formed again, but this time the process is disrotatory.

If, instead of considering only the first isomer formed, the reaction is allowed to continue, then many rotations follow each other. Thus, a given initial distribution of energy leads to the molecule passing successively through the neighborhoods of many isomers (cis and trans). Since the starting molecule is a cis isomer, it is appropriate to study the variation (as a function of δ) of the ratio

$$R = ([\text{cis}] - [\text{trans}])/N$$

where N = [cis] + [trans], and, for instance, [cis] denotes the number of times the cis geometry is reached during the continuous rotations of the methylene groups. In Figure 8b N is limited to 3, and to 7 in Figure 8c. R = 1 (−1) means that only cis (trans) isomers are reached during the rotations. A value of R close to zero corresponds to the following situation: for the initial energy distribution, the dynamical trajectory goes successively through the neighborhood of isomers of the two types, with about the same probability. The tendency of R to oscillate around zero with a small amplitude appears already in Figure 8b where N = 3. It is more clearly confirmed in Figure 8c where N = 7. One observes that the values of δ very close to 45° and the value δ = −45° only lead to the cis isomer being reached exclusively (R = 1); for all the other values of δ, both isomers are reached with about the same rate ($R \sim 0$). This means that the initial distribution of the energy, within a wide range of δ, does not influence notably which isomer is formed.

Now, all the trans isomers are geometrical isomers of the cis starting molecule. They form a set of two enantiomers, T(+) and T(−), according to which terminal group has rotated by 180°. On the other hand, a cis isomer reached during the rotations can be identical with either the starting molecule [C(+) → C(+)] or its enantiomer [C(+) → C(−)]. Thus, one-half of the cis isomers are indistinguishable from the starting molecule. In the counting process for formation of geometrical and optical isomers, the former are therefore favored by a factor of 2.[12d] If only a single rotation is allowed, the process C(+) → C(+) disappears, and all the cis isomers formed are optical isomers of the starting molecule.

Our dynamical results are strongly dependent on the particular value E_0 = 5.8 kcal/mol of the total energy. For energies smaller than 4 kcal/mol, all the trajectories are nonreactive since none of the two transition states can be attained. For E_0 lying between 4.0 and 4.8 kcal/mol, the trajectories may either lead to the optical isomer (for δ close to 45°) or be nonreactive. Finally, for E_0 greater than 4.8 kcal/mol, both isomerizations can be observed. However, for E_0 just above the threshold of 4.8 kcal/mol, the optical isomerization remains the privileged reaction process, and nonreactive trajectories are still numerous ($\delta < 0$). As soon as the excess energy is greater than 1 kcal/mol, the first rotation is always reactive and both isomers (optical and geometrical) can be formed (*cf.* Figure 8a).

It is important to note that none of the initial conditions allow for a dynamical trajectory following the static reaction path proposed[9] for the geometrical isomerization. Indeed, the simplest dynamical pathway through the geometrical col [disrotatory, conrotatory, disrotatory (Figure 7e)] is exactly opposite to the static minimum-energy path [conrotatory, disrotatory, conrotatory]. We explain this result as follows: When the initial rotational motion of the two groups is conrotatory, nothing on the surface (as a bump, for instance) can block the rotation of one of the two groups, while the rotation of the other group goes on. An initial conrotatory motion therefore leads necessarily to the formation of the *optical* isomer. However, a slight modification in the initial position of the two rotors (determined by the values of θ_1^0 and θ_2^0) can produce dynamical trajectories so that the molecule reaches directly the transition state, and the reaction coordinate is locally disrotatory as anticipated. The same result is observed, for initial conditions $\theta_1^0 = \theta_2^0 = 0$, if the representative point of the molecule is left free to move on the surface as long as needed (complex trajectory) for suitable values of $\{\theta_1, \theta_2, \dot{\theta}_1, \dot{\theta}_2\}$ being produced, which makes possible passage of the col along a local disrotatory coordinate (see Figure 7d).

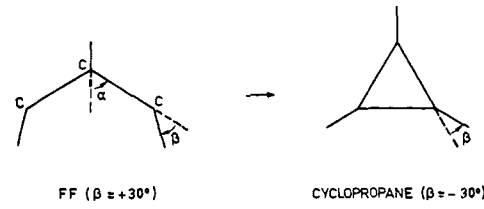

Figure 9. Definition of the two geometrical parameters (angles α and β) primarily concerned in the ring closure from the diradical FF to cyclopropane.

(c) Influence of Substituents. From the set of equations (1) it appears that the multiplication of the moment of inertia I by a constant F, all other things being equal, simply multiplies the durations of the rotations by $F^{1/2}$. In the replacement of the terminal hydrogens of cyclopropane by methyl groups (tetramethylcyclopropane), $F^{1/2}$ equals 5.8. In this case, and for given initial conditions, the substitution does not alter the shapes of the trajectories but lengthens the duration of the rotational motion by a factor of 6. Obviously, this is only a very rough approximation since this result is based on the assumption that the potential-energy surface for the two rotations of the terminal groups is the same for cyclopropane and tetramethylcyclopropane.

Ring Closure of the Face-to-Face (FF) Diradical

1. Description of the Computed Potential-Energy Surface. The motion of ring closure from the face-to-face diradical FF to cyclopropane involves essentially two important geometrical parameters: the angle of ring opening, denoted by 2α, which varies from 113 to 60°, and the angle between the projection of C–H bonds in the CCC plane and the adjacent C–C bond, which define the pyramidalization of the terminal methylene groups (Figure 9). This angle (denoted by β) is −30° in the cyclopropane. In FF, the energy is minimal for β = +30°;[19] *i.e.*, the methylene groups are pyramidalized toward the inner part of the ring (see Figure 9). The two-dimensional (2α,β) potential-energy surface is pictured in Figure 10, along with the minimum-energy path (drawn approximately) which is bent. In the first part of this path, the terminal methylene groups tend to keep the same inward pyramidalization; inversion occurs only in the second part of the path. The strong curvature of the minimum-energy path will create centrifugal effects due to which all the dynamical trajectories deviate (more or less) from this static path.

2. Analytical Expression of the Potential-Energy Function. The computed potential-energy surface appears rather complicated: the reaction coordinate is not rectilinear, and there is no symmetry element in the surface (Figure 10). Thus it is difficult to find *a priori* a simple analytic formula, as a function of α and β, which reproduces the main features of the surface. A

(19) Y. Jean and L. Salem, *Chem. Commun.*, 382 (1971).

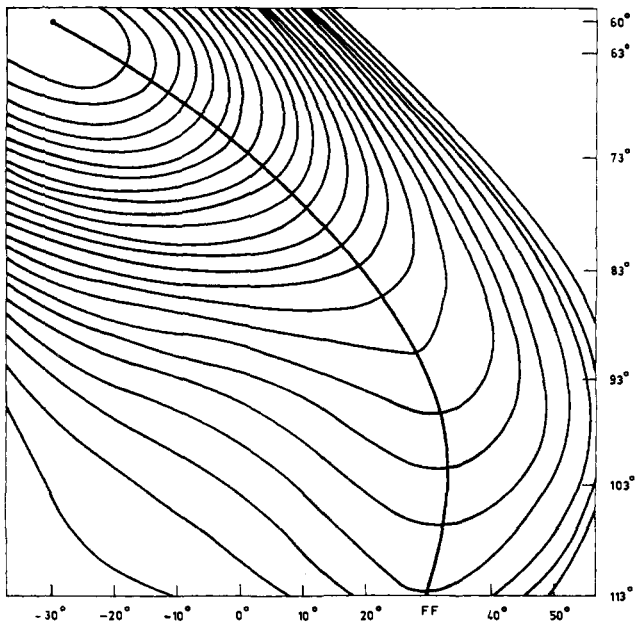

Figure 10. Static reaction path for the ring closure from FF to cyclopropane. The abscissas are the values of the angle β, the ordinates the values of the angle 2α. The energy gap between two isoenergetic lines is 2.5 kcal/mol.

general technique of interpolation of computed values of the potential must be used. The following method makes use of cubic polynomial functions called splines. The technology and the application to the analytic description of potential-energy surfaces are developed in ref 8.

3. Equations of Motion and Initial Conditions. The equations of motion for the problem are established as an application of the theory of constrained systems.[8] The notations for the geometrical parameters and for the masses are shown in Figure 11. Otherwise, the quantities $A_{\alpha\alpha}$, $A_{\alpha\beta}$, and $A_{\beta\beta}$ are the elements of the symetric matrix **A** defined formally in ref 8.

It would require five degrees of freedom (α, β, L, λ, and λ') to treat the problem with no constraint except the required symmetry with respect to (i) the plane of the ring and (ii) the bisecting plane perpendicular to the ring. Here the three lengths L, λ, and λ' are frozen, and the problem is studied in only two dimensions, α and β. Consequently, the present system is *highly constrained.* The reduction, from five dimensions to two, results in the following **A** matrix

$$A_{\alpha\alpha} = A + B + C$$
$$A_{\alpha\beta} = -(A + B/2)$$
$$A_{\beta\beta} = A$$

where

$$A = 2(2m_1)\lambda^2\left\{1 - \frac{\rho}{1+\rho}\frac{2m_1}{M+2m_1}\sin^2(\alpha - \beta)\right\}$$

$$B = \frac{2}{1+\rho}(2m_1)L\lambda\{(2+\rho)\cos\beta + \rho\cos(2\alpha - \beta)\}$$

$$C = \frac{2}{1+\rho}(M+2m_1)L^2\{1 + \rho\cos^2\alpha\}$$

$$\rho = 2\frac{M+2m_1}{M+2m_2}$$

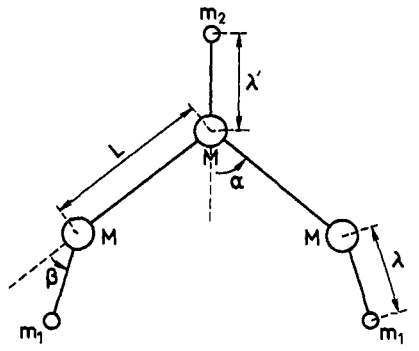

Figure 11. Definition of the geometrical parameters (variable angles and constant bond lengths) and the masses.

The elements of the inverse matrix $\mathbf{A}^{-1}$ are consequently

$$A_{\alpha\alpha}^{-1} = A/D$$
$$A_{\alpha\beta}^{-1} = (A + B/2)/D$$
$$A_{\beta\beta}^{-1} = (A + B + C)/D$$

where $D = AC - B^2/4$.

We introduce the quantities

$$E = \frac{2\rho}{1+\rho}(2m_1)L\lambda\sin(2\alpha - \beta)$$

$$F = -\frac{2+\rho}{1+\rho}(2m_1)L\lambda\sin\beta$$

$$G = \frac{2\rho}{1+\rho}\frac{(2m_1)^2}{M+2m_1}\lambda^2\sin(2\alpha - 2\beta)$$

$$H = -\frac{2\rho}{1+\rho}(M+2m_1)L^2\sin 2\alpha$$

Then we have

$$\frac{\partial A_{\alpha\alpha}}{\partial\alpha} = -2E - G + H \qquad \frac{\partial A_{\alpha\alpha}}{\partial\beta} = E + 2F + G$$

$$\frac{\partial A_{\alpha\beta}}{\partial\alpha} = E + G \qquad \frac{\partial A_{\alpha\beta}}{\partial\beta} = -\left(\frac{E}{2} + F + G\right)$$

$$\frac{\partial A_{\beta\beta}}{\partial\alpha} = -G \qquad \frac{\partial A_{\beta\beta}}{\partial\beta} = G$$

For the Lagrangian equations, we first write the components of the vector **S**

$$S_\alpha = \frac{1}{2}\frac{\partial A_{\alpha\alpha}}{\partial\alpha}\pi_\alpha^2 + \frac{\partial A_{\alpha\alpha}}{\partial\beta}\pi_\alpha\pi_\beta + \left[\frac{\partial A_{\alpha\beta}}{\partial\beta} - \frac{1}{2}\frac{\partial A_{\beta\beta}}{\partial\alpha}\right]\pi_\beta^2 + \frac{\partial U}{\partial\alpha}$$

$$S_\beta = \left[\frac{\partial A_{\alpha\beta}}{\partial\alpha} - \frac{1}{2}\frac{\partial A_{\alpha\alpha}}{\partial\beta}\right]\pi_\alpha^2 + \frac{\partial A_{\beta\beta}}{\partial\alpha}\pi_\alpha\pi_\beta + \frac{1}{2}\frac{\partial A_{\beta\beta}}{\partial\beta}\pi_\beta^2 + \frac{\partial U}{\partial\beta}$$

and finally

$$\begin{aligned}\dot{\alpha} &= \pi_\alpha \\ \dot{\pi}_\alpha &= -[A_{\alpha\alpha}^{-1}S_\alpha + A_{\alpha\beta}^{-1}S_\beta] \\ \dot{\beta} &= \pi_\beta \\ \dot{\pi}_\beta &= -[A_{\alpha\beta}^{-1}S_\alpha + A_{\beta\beta}^{-1}S_\beta]\end{aligned} \tag{3}$$

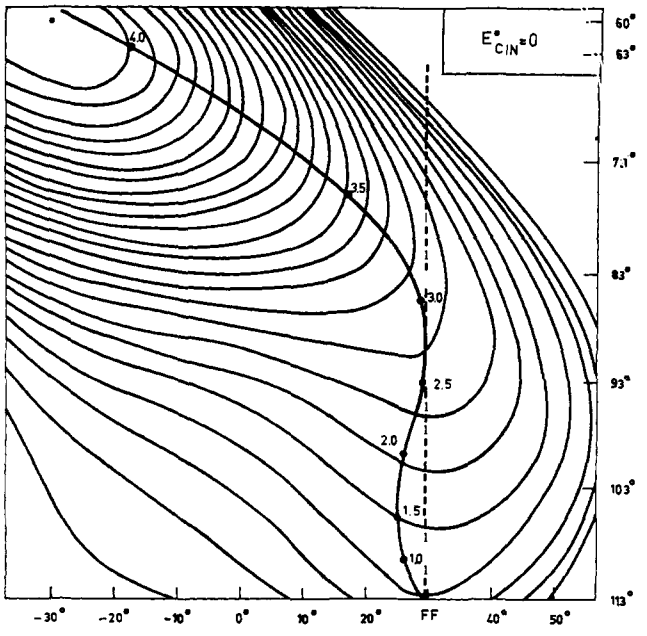

Figure 12. The basic trajectory for the ring closure of unsubstituted cyclopropane with zero kinetic energy in the opened-ring configuration FF.

The numerical integration of the four coupled first-order differential equations (3) requires four initial conditions. These are (i) the values α^0 and β^0 which determine the molecular geometry at the starting point [the trajectories presented below, which describe ring closure processes for the diradical FF, all correspond to the same starting point: $\alpha^0 = 113°/2 = 56.5°$ and $\beta^0 = +30°$]; (ii) the initial kinetic energy E_0 of the molecule as it *starts to reclose* from FF [since the energy of the diradical FF is only slightly below that of the transition states, the initial value of the kinetic energy is varied within the narrow range 0 to 5 kcal/mol]; (iii) the manner in which E_0 is distributed between the modes of reclosure and the mode of depyramidalization. This is defined by an angle (Δ) such that

$$tg\Delta = \beta^0/\dot{\alpha}^0$$

Δ is the angle between the initial velocity vector and the straight line $\beta = \beta^0$ in Figure 12. It defines unequivocally $\dot{\alpha}^0$ and $\dot{\beta}^0$; for instance

$$\dot{\alpha}^0 = -\left[\frac{2\{E_0 - V(\alpha^0,\beta^0)\}}{A_{\alpha\alpha}(\alpha^0,\beta^0) + 2A_{\alpha\beta}(\alpha^0,\beta^0)tg\Delta + A_{\beta\beta}(\alpha^0,\beta^0)tg^2\Delta}\right]^{1/2}$$

For each value of $E_0 = 0$, 1, 3, or 5 kcal/mol, ten trajectories were run for ten different Δ's between -90 and $+90°$, with a step size of 20°.

4. Results. (a) Cyclopropane. Our model does not make possible either a deactivation of the molecule by collision or an energy transfer to a nonreactive mode. Thus, if a trajectory is integrated through a sufficient length of time, there occurs a sequence of ring-closure and ring-opening processes. In fact, for the trajectories presented below, the integration is stopped whenever the representative point of the molecule enters a prescribed narrow neighborhood of cyclopropane in its equilibrium geometry. Then deactivation would lead to a vibrationally unexcited cyclopropane molecule.

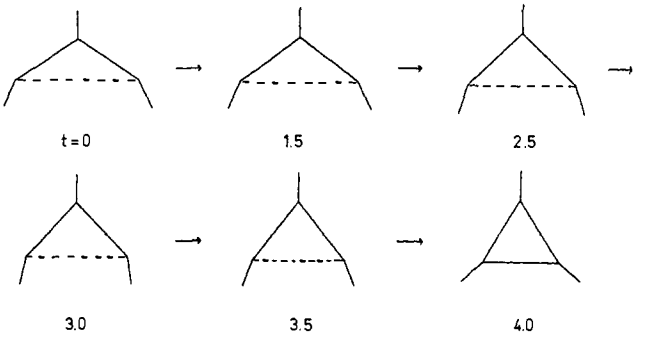

Figure 13. Projection on the CCC plane of the motion of the nuclei through time, in the course of ring closure for unsubstituted cyclopropane ($E^0_{cin} = 0$).

In Figure 12, we represent the trajectory for vanishing initial kinetic energy ($E_0 = 0$). It is probably the trajectory which best matches the static minimum-energy path, at least at the beginning. Indeed, the forms of the two curves in Figures 10 and 12 are in rather good conformity. However, their superposition brings out two differences: (i) The form of the static reaction path close to the starting point (α^0, β^0) is somewhat different from the dynamical trajectory. This indicates clearly again, if still necessary, that predictions from static reaction paths on potential-energy surfaces are very limited and somewhat dangerous, particularly in rather flat regions. (ii) That part of the trajectory where terminal methylene groups remain pyramidalized toward the inside of the ring is longer than the same fraction of the minimum-energy path. This is a purely dynamical effect due to the molecular motion being unable to adjust instantaneously to the changes of curvature of the equipotential lines (because of centrifugal forces). In Figure 13, the projection on the plane of the carbons of the displacements of the different atoms in the course of the cyclization is represented.

The ring closure occurs in 4.13×10^{-14} sec. It is noticeable that the motion starts very slowly because of the weak force (the gradient of a rather flat surface) acting on the angle CCC. Thus, half the time (2.0×10^{-14} sec) is devoted to the angle decreasing from 113 to 100° only. The rather long time spent by the representative point of the molecule in the region of the surface where the rotation of one or both methylene groups is still possible, *i.e.*, without requiring an unrealistic amount of energy, may have important mechanistic consequences. Indeed, this time interval should be sufficient for a methylene group with a few kilocalories in its rotational mode to rotate by a large angle (40 to 50°). Now such a rotation can block the reclosing motion and allow for supplementary rotations in the diradical. The introduction of the coupling between ring closure and rotation should bring definitive information on this particular point.

When the diradical FF has initially a small amount of excess energy in either its reclosing mode or its depyramidalization mode, or both, the dynamical trajectories deviate only slightly from the fundamental trajectory described previously. Figure 14 shows three trajectories for $E_0 = 5$ kcal/mol and $\Delta = +70$, $+10$, and $-50°$. The ring-closure process is now faster than for $E_0 = 0$ (about 2.75×10^{-14} sec, whatever Δ). In contrast with the high sensitivity of the rotational trajec-

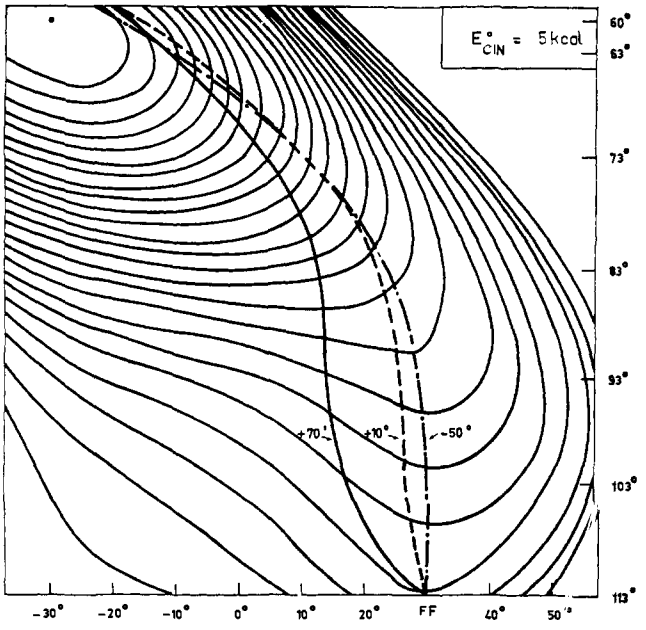

Figure 14. Some typical dynamical trajectories for the ring closure of unsubstituted cyclopropane in the case of nonzero initial kinetic energy (E^0_{cin} = 5 kcal/mol) and various distributions of this energy.

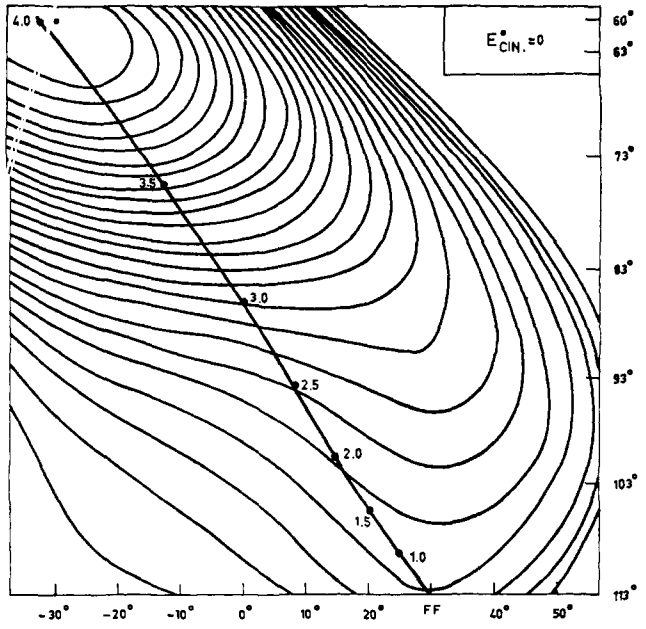

Figure 15. The basic dynamical trajectory for the ring closure of heavily substituted cyclopropane (1,1,2,2-tetramethylcyclopropanef with zero kinetic energy in the opened-ring configuration FF.

tories to the initial conditions, the shape of the ring-closure trajectories is rather insensitive to the initial conditions over a wide range; the gap between the static reaction path and the dynamical trajectories remains small. This is mainly due to the sharp steepness of the surface, whereas the rotational surface is rather flat. Finally, let us note that the direction of the trajectories in the region around the representative point of cyclopropane (the absolute minimum of the surface) also indicates the best energetic distribution for the reverse reaction, *i.e.*, for the ring opening of cyclopropane to the diradical FF. The static pathway is actually a good approximation to these dynamic pathways.

(b) Substituted Cyclopropanes. Trajectories were also run for 1,1,2,2-tetramethylcyclopropane and for hexamethylcyclopropane. The same potential-energy surface was used. This seems reasonable on the basis of quantum-mechanical calculations on the 1,2-dimethylcyclopropane molecule, which show that substitution of hydrogens by methyl groups does not alter significantly the main features of the ring closure potential-energy surface,[16] particularly for pyramidalization of the terminal groups. The most important result is that the time required by the ring-closure process is only slightly affected by the nature of substituents. For instance, for $E_0 = 0$ this time is 4.0×10^{-14} sec for 1,1,2,2-tetramethylcyclopropane. The corresponding trajectory is pictured in Figure 15. This is due to the fact that the dynamical trajectories for the ring closure of substituted cyclopropanes are almost straight lines, *i.e.*, are *shorter* than the bent trajectories obtained for unsubstituted cyclopropane under the same initial conditions. As the velocities are smaller, however, in the heavier substituted molecules, the overall duration of the process is the same. Now, we saw how sensitive rotation times are to the mass of the substituent groups on the terminal carbons (they are enhanced by a factor of 6 when replacing the cyclopropane by the 1,1,2,2-tetramethylcyclopropane). Therefore, substitution should favor cyclization relative to rotation. It is only as long as the ring is suitably opened that a rotation can occur. If the rotational distortion with respect to the FF conformation remains small (as should often be the case for heavily substituted cyclopropanes), the ring-closure process can occur before any transition state is reached. Qualitatively, this is observed in experiments where reaction rates are measured for disubstituted and tetrasubstituted cyclopropanes. The ratio k_{cyc}/k_{rot} of the reaction rates for cyclization and rotation is equal to $^1/_5$ for 1-methyl-2-ethylcyclopropane[12c] and to 11 for tetramethylcyclopropane-d_6.[12b] The experimental study of the pyrolysis of substituted cyclobutanes leads to a similar result. These reactions involve the 1,4-butanediyl diradical intermediate, which subsequently leads either to olefins through the breaking of the C_2–C_3 bond (rate constant, k_d) or to geometrical isomers of the reactant through rotations around the bonds C_1–C_2 or C_3–C_4 followed by cyclization (rate constant, k_i). Heavy substituent groups on the terminal carbons make the ratio k_d/k_i increase.[20] Therefore, substitution again disfavors the reaction process involving rotations around carbon–carbon bonds.

Acknowledgments. The authors are very much indebted to Professor Lionel Salem who initially suggested the study presented here and took a keen interest in its development.

(20) J. A. Berson, D. C. Tompkins, and G. Jones, *J. Amer. Chem. Soc.*, 92, 5799 (1970).